Tellus (1986), *38A*, 366–377

On the dynamics of mid-latitude synoptic systems with intense cumulus convection

By JOCELYN MAILHOT* and MAN KONG YAU, *Department of Meteorology, McGill University, Montréal, Québec, Canada, H3A 2K6*

(Manuscript received March 12; in final form November 29, 1985)

ABSTRACT

A scale analysis appropriate for mid-latitude explosive cyclones is presented, including the effects of cumulus clouds. First-order equations are derived for the thermodynamic and vorticity fields. It is shown that the quasi-geostrophic form of the divergence equation is a good approximation, while the geostrophic wind approximation is no longer valid in the presence of intense convection. It is also found that diabatic heating by clouds is responsible for the enhancement of the large-scale vertical motion which induces a divergent wind on the same order as the rotational part. Therefore, cumulus convection affects the large-scale flow through an induced secondary circulation, which manifests its effect in the thermodynamic and vorticity equations as the advection by the divergent wind component. In addition, cumulus clouds also affect the large-scale vorticity by imparting excess cloud vorticity to the environment.

Interactions between cloud and large scales are also discussed in terms of the omega and potential vorticity equations. It is shown that the dominant forcing terms, i.e. diabatic heating and vortex stretching due to cumulus clouds, tend to balance in the large-scale potential vorticity equation, and that the influence of cumulus convection appears through the smaller forcings due to cloud life-cycles and two non-geostrophic effects.

A three-level model is employed to investigate the effects of cumulus convection on baroclinic instability, with Ekman-CISK as the closure condition. It is found that the various forcing mechanisms produce quite different effects on the evolution and structure of the baroclinically unstable waves.

1. Introduction

In the past two decades, much effort has been devoted to the study of the interactions between cumulus ensembles and the large-scale flow. Most of the studies were concerned with the thermodynamic effects of clouds in tropical regions, where the heating due to latent heat release is believed to play a crucial role in driving the tropical circulations (Riehl and Malkus, 1958). A number of parameterization schemes have been proposed to account for these thermal effects (e.g., Ooyama, 1971; Yanai et al., 1973; Arakawa and Schubert, 1974; Kuo, 1965, 1974; and Cho, 1977). More recently, attention has been directed toward a theoretical formulation of the dynamical effects of cumulus ensembles (Stevens et al., 1977; Shapiro, 1978; Shapiro and Stevens, 1980; Cho et al., 1979; Cho and Cheng, 1980, hereafter referred to as CC). Diagnostic studies of tropical systems during GATE (GARP Atlantic Tropical Experiment) and investigations of synoptic-scale waves in the tropics served as tests for these theories of dynamical interactions. In particular, Stevens et al. (1977) showed that the vertical momentum transport by cumulus convection exerts a damping effect which affects significantly the dynamics of tropical waves. Cumulus friction was found necessary to account for the relatively small amplitude of temperature change given the relatively large heating rate typical of the observed systems.

* Present affiliation: Recherche en Prévision Numérique, Atmospheric Environment Service, Dorval, Québec, Canada, H9P 1J3

The influence of cumulus clouds is by no means limited to the tropics. In recent years, there has been an increase in interest in understanding the role of organized cumulus convection in mid-latitude systems, examples of which are the explosive coastal winter storms and mesoscale circulations such as polar lows and convective complexes. Although the effect of cumulus convection in mesoscale systems is still a matter of debate, there is ample evidence that explosive cyclones are baroclinic events influenced strongly by clouds. Sanders and Gyakum (1980) in a study of explosive cyclones in the Northern Hemisphere over a three-year period, concluded that the behavior of these storms departs appreciably from quasi-geostrophic theory and that their development is strongly and perhaps crucially aided by some forcing mechanisms such as cumulus convection. Case studies (Palmén, 1958; Danard, 1964; Krishnamuri and Moxim, 1971; Tracton, 1973; Bosart, 1981; Gyakum, 1983) yield further evidence on the role of convection in extratropical cyclones.

From the results of these studies, some common features of explosive cyclones have emerged. In these systems, the mean divergence is typically large and is on the same order as the large-scale vorticity. The mean vertical motion is one order of magnitude larger than usual and reaches maximum values on the order of 10^{-2} mb s^{-1}. There are strong convective activities as deduced from surface, radar, and satellite reports. The precipitation rates are on the order of 10 cm day^{-1}, although it is not clear how much is associated with stratiform clouds.

Because of the strong coupling between thermodynamics and dynamics in a quasi-geostrophic system, the effects of cumulus convection on the large scale should not be limited to diabatic heating alone. Some evidence for the dynamical importance of convection comes from kinetic energy budget studies (e.g., Vincent and Schlatter, 1979). It has also been suggested by Yip and Cho (1982; hereafter referred to as YC) that the dynamical effects of clouds may be important for quasi-geostrophic systems under certain situations. From a scale analysis of the appropriate equations, they showed that the most important dynamic effect in the large-scale vorticity arises from the divergence of the horizontal eddy flux of vorticity. Using the theory of CC, they interpreted this term as a combination of the ~~cloud~~ life-cycle and an effect due to vortex tube stretching by cumulus ~~clouds~~. In the context of a linear model of quasi-geostrophic baroclinic instability with Ekman-CISK (conditional instability of the second kind), they demonstrated that the growth rate of a baroclinically unstable wave would be increased appreciably by cloud-scale processes. However, their choice of scale for the diabatic heating is more appropriate for weaker systems where the large-scale vertical motion is still given by the quasi-geostrophic theory. Furthermore, their analysis did not treat explicitly the role of the divergent part of the wind which has been shown to play a major role in the kinetic energy budgets (Chen et al., 1978).

The purpose of this paper is to clarify through scale and linear analysis the major effects of cumulus ensembles on mid-latitude synoptic-scale systems with intense convective activities, more specifically the explosive winter cyclones. The analysis is based on typical scales of these systems, and includes both stratiform precipitation and cumulus convection formulated after the parameterization of Cho (1977). It will be shown that the heating inside the clouds increases significantly the large-scale vertical motion, which in turn induces a divergent wind component of the same order of magnitude as the non-divergent wind. The advection by the divergent wind makes important contributions in both the thermodynamic and vorticity equations, and constitutes the basic mechanism by which heating in the clouds influences the large-scale flow. In addition, the recycling rate effect due to the finite life-span of the clouds also contributes to the large-scale vorticity, as was first demonstrated by YC.

In Section 2, a scale analysis of the governing equations is carried out for mid-latitude synoptic-scale systems in the presence of intense convection. The derivation and a discussion of the appropriate potential vorticity and omega equations are in Section 3. Section 4 deals with a baroclinic instability analysis including the effects of clouds, in the context of a three-level model. Finally, Section 5 summarizes the major conclusions.

2. Scale analysis

A scale analysis will be used to derive a consistent set of equations governing explosive cyclones. The basic premise is that the precipitation rate is on the order of 10 cm day^{-1}, which corresponds to a mean diabatic heating rate of 25–30 K day^{-1} for a tropospheric column. It will be shown that this heating rate is only possible in the presence of intense convective activities. In particular, the total cloud vertical mass flux M_c, the fractional cumulus cloud cover Σ, and the mean cloud lifetime τ turn out to be an order of magnitude larger than that assumed by YC.

Our analysis will be brief as it parallels the development given in YC. Unless stated otherwise, the scales chosen will be the same as those given therein. Interested readers can refer to that article and Mailhot (1985) for further details.

2.1. *Thermodynamic equation*

The large-scale thermodynamic equation, including the effects of cumulus and stratiform clouds, is similar to eq. (10) in YC:

$$\frac{\partial\bar{\theta}}{\partial t} + \bar{V}\cdot\nabla\bar{\theta} + \bar{\omega}\frac{\partial\bar{\theta}}{\partial p} = -M_c\frac{\partial\bar{\theta}}{\partial p} + \frac{Q_s}{c_p\pi} \tag{2.1}$$

Here the overbar denotes a horizontal areal average, Q_s is the contribution from the stratiform clouds, and $\pi = (p/1000)^{R/c_p}$.

Recent diagnostic studies by Bosart (1981) and Gyakum (1983) indicated that, on the average, the temperature variation in rapidly deepening disturbances does not exceed about 5 K day^{-1}. However, in the same works and earlier investigations by Palmén (1958) and Danard (1964) it was found that a typical diabatic heating rate is on the order of 25 to 30 K day^{-1}. Therefore, to maintain a relatively small temperature change in the presence of a large diabatic heating, there must be a balance on the whole by adiabatic cooling due to large-scale upward motion. This indicates that in these systems the large-scale vertical velocity is

$$\bar{\omega} \sim 10^{-2}\ \text{mb s}^{-1}.$$

For the stratiform component, we adopt a simple parameterization (e.g., Haltiner, 1971, Chap. 9; Krishnamurti and Moxim, 1971)

$$Q_s = -L\tilde{\omega}\frac{\partial\bar{q}_{sat}}{\partial p},$$

where $\bar{q}_{sat}$ denotes the saturation specific humidity. Here a variable with a tilde refers to its value in the cumulus cloud environment, which contains the stratiform clouds.

Using the conservation of mass over a horizontal area in the form

$$\tilde{\omega} = \bar{\omega} + M_c \tag{2.2}$$

and defining an effective stability parameter σ_e which includes the effects of the stratiform clouds (e.g., Krishnamurti, 1968)

$$\sigma_e = -\frac{R\pi}{p}\left(\frac{\partial\bar{\theta}}{\partial p} + \frac{L}{c_p\pi}\frac{\partial\bar{q}_{SAT}}{\partial p}\right),$$

we can write (2.1) as:

$$\frac{\partial\bar{\theta}}{\partial t} + (\bar{V}_\psi + \bar{V}_\chi)\cdot\nabla\bar{\theta} - \tilde{\omega}\frac{p\sigma_e}{R\pi} = 0. \tag{2.3}$$

This is the first-order thermodynamic equation applicable to mid-latitudes synoptic systems with intense convection. It is expressed here in terms of the mean vertical velocity in the cloud environment and is similar to eq. (38) of YC. However, in the present case the horizontal advection by the divergent wind is retained as it is on the same order as the other terms. It can be shown readily from the scaling of the continuity equation, using $\bar{\omega} \sim 10^{-2}$ mb s^{-1}, that the divergent and rotational parts of the wind are of the same order. This result is in agreement with observations that the magnitudes of the large-scale divergence and vorticity in such systems are quite similar.

From (2.3) it can further be shown that (e.g., YC, eq. 27)

$$\tilde{\omega} \sim 10^{-3}\ \text{mb s}^{-1}.$$

Thus the vertical motion in the environment $\tilde{\omega}$ is one order of magnitude smaller than $\bar{\omega}$. According to (2.2), this indicates that the large-scale vertical velocity $\bar{\omega}$ is mainly associated with the total vertical mass flux M_c inside cumulus clouds, similar to the case of convectively active regions in the tropics discussed in Holton (1979). Therefore, the following scale is obtained for M_c.

$$M_c \sim 10^{-2}\ \text{mb s}^{-1}.$$

2.2. *Vorticity equation*

The large-scale vorticity equation in the presence of convection can be written as:

$$\frac{\partial \bar{\zeta}}{\partial t} + \bar{V}\cdot\nabla(\bar{\zeta}+f) - (\bar{\zeta}+f)\frac{\partial \bar{\omega}}{\partial p} + M_c\frac{\partial \bar{\zeta}}{\partial p} + k\cdot\nabla\bar{\omega} \times \frac{\partial \bar{V}}{\partial p} = -\nabla\cdot\overline{V'\eta'} - k\cdot\nabla\times\left(\overline{\omega'\frac{\partial V'}{\partial p}}\right). \tag{2.4}$$

A scale analysis of (2.4) indicates that the term $f\partial\bar{\omega}/\partial p$ is one order of magnitude larger than any term on the left-hand side, and that it can only be balanced by the divergence of the horizontal eddy flux of vertical vorticity $\nabla\cdot\overline{V'\eta'}$. Therefore the zeroth-order approximation to the vorticity equation is

$$f\nabla\cdot\bar{V}_\chi = -\nabla\cdot\overline{V'\eta'}. \tag{2.5}$$

Furthermore, according to the scaling proposed by YC and CC for $\nabla\cdot\overline{V'\eta'}$, (2.5) implies that $\Sigma \sim 10^{-1}$, which is one order of magnitude larger than that assumed in YC.

It should be remarked that this scale for Σ is consistent with the scale for M_c. Following YC, M_c is defined as

$$M_c = \Sigma\bar{\rho}g\bar{w}_c$$

where $\bar{w}_c$ is the vertical velocity of the clouds averaged over the ensemble and has a magnitude of 1 m s^{-1} here. YC pointed out that the slice method provides an upper bound for Σ on the order of 10–20%, depending on the thermal stratification of the atmosphere. They showed that it is consistent to choose $\Sigma \sim 1\%$ of the total area if the magnitude of M_c is around 10^{-3} mb s^{-1}. Since M_c is ten times larger in the present case and $\bar{w}_c$ is not expected to vary by an order of magnitude, it seems reasonable to have $\Sigma \sim 10\%$.

The remaining terms in (2.4) are first-order terms. However some simplification is possible when a specific cumulus cloud parameterization is introduced. Following CC, the apparent vorticity source Z defined by the right-hand side of (2.4) can be expressed as:

$$Z = \frac{\Sigma}{\tau}(\bar{\eta}_c - \bar{\eta}) + (\bar{\zeta}+f)\frac{\partial M_c}{\partial p} - M_c\frac{\partial \bar{\zeta}}{\partial p} - k\cdot\nabla M_c \times \frac{\partial \bar{V}}{\partial p},$$

where $\bar{\eta}_c$ is the mean absolute vorticity over cloud areas. The first term is usually referred to as the cloud life-cycle effect because Σ/τ can be interpreted as the recycling rate of atmospheric air by cumulus convection (Cho, 1977) while $\bar{\eta}_c - \bar{\eta}$ represents the net increase of vorticity over cloud areas. The other terms represent respectively the vortex tube stretching by the clouds, the vertical advection of vorticity due to the vertical mass flux of the cloud ensemble, and the twisting effect due to the inhomogeneous spatial distribution of the cloud population. A similar expression for the apparent vorticity source was obtained by Shapiro and Stevens (1980), using a bulk cloud model based on a steady-state one-dimensional entraining jet. In their formulation, the first term is interpreted as a source due to the detrainment of cloud substance into the environment.

Using the form of Z in (2.4), together with (2.2), the first-order vorticity equation applicable to synoptic systems in the presence of intense convection turns out to be

$$\frac{\partial \bar{\zeta}}{\partial t} + (\bar{V}_\psi + \bar{V}_\chi)\cdot\nabla(\bar{\zeta}+f) - f\frac{\partial \bar{\omega}}{\partial p} = \frac{\Sigma}{\tau}(\bar{\eta}_c - \bar{\eta}). \tag{2.6}$$

(2.6) is similar to eq. (39) in YC, except for the addition of the vorticity advection by the divergent part of the wind.

The terms on the left-hand side of (2.6) are all of order $\sim 10^{-10}$ s^{-2}. For organized convective systems in the mid-latitudes, the vorticity excess $\bar{\eta}_c - \bar{\eta} \sim 10^{-5}$ s^{-1} (Cho et al., 1979). Using $\Sigma \sim 10^{-1}$ or less, it follows that τ must be $\sim 10^4$ s in order for

$$\frac{\Sigma}{\tau}(\bar{\eta}_c - \bar{\eta}) \leqslant 10^{-10}\ \text{s}^{-2},$$

so that it is consistent with the magnitudes of the terms on the left-hand side. Note that the value deduced for the mean cloud lifetime agrees well with an advective time scale for the cloud ensemble: $\tau \sim D_c/\bar{w}_c \sim 10^4$ s, where $D_c \sim 10^4$ m, a typical vertical length scale for deep convective clouds.

2.3. *Divergence equation*

To close our system of equations, we need a simplified form of the divergence equation. Although the theory of cumulus parameterization is still incomplete with regard to the diyergencer it can be shown that the quasi-geostrophic approximation

$$f\bar{\zeta} = \nabla^2\bar{\Phi} \tag{2.7}$$

remains valid as a zeroth-order approximation to the complete divergence equation for synoptic-scale systems, even in the presence of intense convection.

From Haltiner (1971, p. 60), the large-scale divergence equation can be written as:

$$\frac{\partial\bar{\delta}}{\partial t} + \nabla\cdot(\bar{V}\bar{\delta}) + \nabla\cdot\left(\bar{\omega}\frac{\partial\bar{V}}{\partial p}\right) - 2J(\bar{u},\bar{v}) + (\boldsymbol{k}\times\bar{V})\cdot\nabla f - f\bar{\zeta} + \nabla^2\bar{\Phi} = -\nabla\cdot\overline{V'\delta'} - \nabla\cdot\overline{\omega'\frac{\partial V'}{\partial p}} + 2\overline{J(u',v')}. \tag{2.8}$$

Even when $V_\chi \sim V$, the largest terms on the left-hand side are still $f\bar{\zeta}$ and $\nabla^2\bar{\Phi}$. A scaling of the eddy terms in (2.8) indicates that only the first term which contains the horizontal eddy flux of divergence can possibly contribute to the zeroth-order approximation. However, it can easily be shown from the areal average of the cloud-scale continuity equation that this term is on the order of $\sim 10^{-10}\ \mathrm{s}^{-2}$, and can be neglected to zeroth order.

Thus the usual quasi-geostrophic scaling for the pressure force is still valid. It is generally observed that the geopotential gradients are somewhat larger in the kind of systems considered here but by no means differ from quasi-geostrophic systems with weaker convection by one order of magnitude.

The zeroth-order approximation to (2.8) can be written in terms of the streamfunction as

$$f\nabla^2\bar{\psi} = \nabla^2\bar{\Phi}. \tag{2.9}$$

Therefore the usual relation between the streamfunction and the geopotential is a good approximation even for explosive cyclones.

2.4. Horizontal momentum equation

A scaling of the horizontal equation of motion shows that when $\Sigma \sim 10^{-1}$ the zeroth-order approximation to the horizontal momentum equation is generally given by:

$$f\boldsymbol{k}\times\bar{V} = -\nabla\bar{\Phi} - \boldsymbol{k}\times\overline{V'\eta'}. \tag{2.10}$$

By using (2.5) and (2.9), (2.10) can be partitioned into a rotational and a divergent component as

$$f\boldsymbol{k}\times\bar{V}_\psi = -\nabla\bar{\Phi} \tag{2.11}$$

$$f\bar{V}_\chi = -\overline{V'\eta'}. \tag{2.12}$$

These relations follow directly from the fact that the horizontal eddy flux of vorticity is due entirely to its divergent component $\overline{V'_\chi\eta'}$. CC showed that $\overline{V'_\psi\eta'} \equiv 0$ and this is supported by the numerical results of Cho and Clark (1981). Eq. (2.12) holds strictly as a zeroth-order approximation only in the case where $\Sigma \sim 10^{-1}$. Otherwise the first-order terms in the horizontal equation of motion are also important in the determination of $\bar{V}_\chi$.

(2.10)–(2–12) describe some unique features for explosive synoptic systems. First, the presence of intense convection can create a kind of three-way balance between the large-scale Coriolis and pressure forces and the eddy Coriolis force. Second, the geostrophic wind is no longer a good approximation as there can be an important ageostrophic component generated by cumulus clouds from the horizontal eddy flux of vertical vorticity $\overline{V'\eta'}$. These conclusions are independent of any parameterization scheme; they depend only on our choice of the cloud scales which are consistent with observations.

3. Omega and potential vorticity equations

It is often easier to discuss physical mechanisms in terms of the potential vorticity equation governing the evolution of the flow and the diagnostic omega equation which relates the vertical velocity field to the structure of the flow and to forcing processes.

Dropping the overbar from the large-scale variables, the first-order vorticity, thermodynamic and continuity equations can be written on a β-plane as a closed set in terms of ψ, ω and the potential function χ, viz.,

$$\left[\frac{\partial}{\partial t} + (\boldsymbol{k}\times\nabla\psi + \nabla\chi)\cdot\nabla\right]\nabla^2\psi + \beta\left(\frac{\partial\psi}{\partial x} + \frac{\partial\chi}{\partial y}\right) - f_0\frac{\partial\omega}{\partial p} = \frac{\Sigma}{\tau}(\eta_c - \eta) + f_0\frac{\partial M_c}{\partial p}, \tag{3.1}$$

$$\left[\frac{\partial}{\partial t} + (\boldsymbol{k} \times \nabla\psi + \nabla\chi)\cdot\nabla\right]\frac{\partial\psi}{\partial p} + \frac{\sigma_e}{f_0}\,\omega$$

$$= -\frac{\sigma_e}{f_0}M_c, \tag{3.2}$$

$$\nabla^2\chi + \frac{\partial\omega}{\partial p} = 0. \tag{3.3}$$

On the right-hand side of (3.1) and (3.2), we identify three terms representing cumulus clouds effects on the large scale. These are the recycling rate effect and the vortex tube stretching by the clouds in the vorticity equation, and the heating effect due to latent release inside the cumulus clouds in the thermodynamic equation.

The potential vorticity equation can be obtained by eliminating the ω terms in (3.1) and (3.2):

$$\left(\frac{\partial}{\partial t} + \boldsymbol{k} \times \nabla\psi\cdot\nabla\right)Q = \frac{\Sigma}{\tau}(\eta_c - \eta)$$

$$-\nabla\chi\cdot\nabla Q - \nabla\frac{\partial\chi}{\partial p}\cdot\nabla\frac{f_0^2}{\sigma_e}\frac{\partial\psi}{\partial p}, \tag{3.4}$$

where the potential vorticity is given by

$$Q = \nabla^2\psi + \frac{\partial}{\partial p}\left(\frac{f_0^2}{\sigma_e}\frac{\partial\psi}{\partial p}\right) + f.$$

By eliminating the time tendencies in (3.1) and (3.2), the omega equation becomes:

$$\frac{\sigma_e}{f_0}\nabla^2\omega + f_0\frac{\partial^2\omega}{\partial p^2} + \nabla\frac{\partial\psi}{\partial p}\cdot\nabla(\nabla^2\chi)$$

$$-\nabla\frac{\partial\chi}{\partial p}\cdot\nabla(\nabla^2\psi + f) = J\left(\frac{\partial\psi}{\partial p}, 2\nabla^2\psi + f\right)$$

$$-\frac{\sigma_e}{f_0}\nabla^2 M_c - \frac{\partial}{\partial p}\left[\frac{\Sigma}{\tau}(\eta_c - \eta) + f_0\frac{\partial M_c}{\partial p}\right]. \tag{3.5}$$

A scale analysis of (3.4) and (3.5) shows that all terms in (3.4) are on the order of $10^{-10}\,\mathrm{s}^{-2}$. In (3.5), four terms have a magnitude of $10^{-12}\,\mathrm{mb}^{-1}\,\mathrm{s}^{-2}$ with the rest at $10^{-13}\,\mathrm{mb}^{-1}\,\mathrm{s}^{-2}$. Thus the zeroth-order equation for (3.5) is

$$\frac{\sigma_e}{f_0}\nabla^2\omega + f_0\frac{\partial^2\omega}{\partial p^2} = -\frac{\sigma_e}{f_0}\nabla^2 M_c - f_0\frac{\partial^2 M_c}{\partial p^2}. \tag{3.6}$$

A physical interpretation of the forcing effects by cumulus convection on the large scale can be made on the basis of (3.4) and (3.6). It is evident from the omega equation that the diabatic heating and the stretching by the cloud ensemble (the two terms containing M_c) provide the strongest forcing to the large-scale vertical motion. In turn, this vertical motion is related to a secondary circulation characterized by a strong divergent wind component. This divergent wind then forces the large-scale potential vorticity through two non-geostrophic terms appearing in (3.4), in addition to the cloud life-cycle effect. It is worth noting that the heating and vortex stretching terms due to the clouds do not appear explicitly in the potential vorticity equation which governs the large-scale flow. In fact, the heating effect is exactly cancelled by the stretching term. Clearly, this has important implications: if only the thermodynamic effects of clouds are included, the forcing on the large-scale potential vorticity would be overestimated. This conclusion is in agreement with the results of Stevens et al. (1977) for tropical waves.

4. Baroclinic instability analysis

Having derived through scale analysis a simplified set of equations appropriate for mid-latitude explosive cyclones, we are in a position to assess the different effects due to cumulus convection on the evolution of these systems. This will be done in the context of a linear baroclinic instability analysis using a three-level model (Fig. 1).

Our starting point is the set of equations (3.1)–(3.3), comprising the vorticity, thermodynamic and continuity equations. These equations are linearized with respect to a zonal westerly flow $U(p)$ having a linear shear in the vertical.

We first partition the total wind as the sum of the zonal part and small perturbations denoted by primes (not to be confused with the notation used in Section 2 for the subscale eddies), viz.

$$\boldsymbol{V}_\psi = \boldsymbol{i}U(p) + \boldsymbol{k} \times \nabla\psi'(x, y, p, t), \tag{4.1}$$

$$\boldsymbol{V}_\chi = \nabla\chi'(x, y, p, t) \tag{4.2}$$

The continuity equation (3.3) together with (4.2) then gives

$$\omega = \omega'(x, y, p, t) \tag{4.3}$$

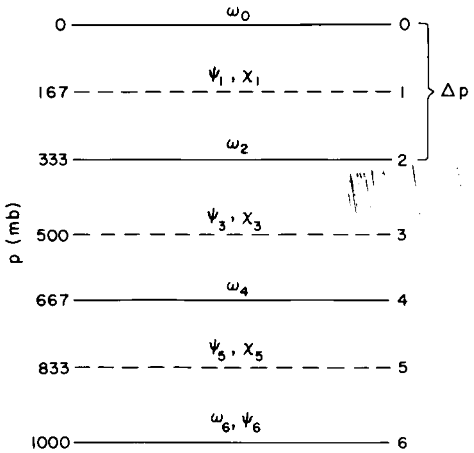

Fig. 1. Arrangement of variables in the vertical for the three-level model.

The expansions (4.1)–(4.2) imply that

$$\psi = \bar{\Psi}(y, p) + \psi'(x, y, p, t), \tag{4.4}$$

$$\chi = \chi'(x, y, p, t), \tag{4.5}$$

$$U(p) = -\frac{\partial \bar{\Psi}}{\partial y}. \tag{4.6}$$

The linearized equations for the disturbance are then

$$\left(\frac{\partial}{\partial t} + U\frac{\partial}{\partial x}\right)\nabla^2\psi' + \beta\left(\frac{\partial \psi'}{\partial x} + \delta\frac{\partial \chi'}{\partial y}\right) - f_0\frac{\partial \omega'}{\partial p} = \frac{\Sigma}{\tau}(\eta_c - \eta) + f_0\frac{\partial M_c}{\partial p}, \tag{4.7}$$

$$\left(\frac{\partial}{\partial t} + U\frac{\partial}{\partial x}\right)\frac{\partial \psi'}{\partial p} - \frac{\mathrm{d}U}{\mathrm{d}p}\left(\frac{\partial \psi'}{\partial x} + \delta\frac{\partial \chi'}{\partial y}\right) + \frac{\sigma_\epsilon}{f_0}\omega' = -\frac{\sigma_\epsilon}{f_0}M_c, \tag{4.8}$$

$$\nabla^2\chi' + \frac{\partial \omega'}{\partial p} = 0, \tag{4.9}$$

where δ is a parameter which can take on value of 0 or 1 to enable us to keep track of the non-geostrophic terms.

To solve this system of equations, we still need a closure condition to relate the cumulus cloud effects to the large-scale variables. For that purpose, we will invoke the CISK mechanism, which assumes the existence of a cooperative interaction between cumulus convection and the large-scale motion (Holton, 1979, Chap. 10), in the form of a feedback to convection by the low-level moisture convergence of the large-scale disturbance. For simplicity, we will adopt the Ekman pumping formulation of Charney and Eliassen (1964). In this model, the low-level convergence is due to the frictionally induced cross-isobaric flow and the vertical velocity at the top of the Ekman layer is simply proportional to the vorticity. We thus assume for the cloud mass flux M_c

$$M_c = -\epsilon h(p)\,\omega'_B. \tag{4.10}$$

For the recycling rate effect of cumulus clouds on the vorticity, we will use a closure condition similar to YC

$$\frac{\Sigma}{\tau}(\eta_c - \eta) = -\varepsilon g(p)\,\omega'_B \tag{4.11}$$

where

$$\omega'_B = -E_k\nabla^2\psi'_B. \tag{4.12}$$

The Ekman parameter E_k depends on the eddy diffusivity in the Ekman layer. ϵ and ε represent a measure of the moisture supply from the moist layer to the convection. The functions $h(p)$ and $g(p)$ denote the vertical distribution of cloud-induced effects.

The next step is to assume normal mode solutions for the disturbance in the form

$$\begin{bmatrix}\psi' \\ \chi' \\ \omega'\end{bmatrix} = \begin{bmatrix}\Psi(p) \\ X(p) \\ \Omega(p)\end{bmatrix}\exp\left[ik(x - ct) + ily\right]. \tag{4.13}$$

Here, k and l are the longitudinal and meridional wave numbers, respectively, and c is the complex phase velocity along the east-west axis. Using (4.13), the linear equations are transformed to a set of ordinary differential equations in the variable p:

$$-ikm^2(U - c)\Psi + i\beta(k\Psi + \delta lX) - f_0\frac{\mathrm{d}\Omega}{\mathrm{d}p} = -\left(\varepsilon g + f_0\epsilon\frac{\mathrm{d}h}{\mathrm{d}p}\right)m^2E_k\Psi_B, \tag{4.14}$$

$$ik(U-c)\frac{d\Psi}{dp} - i\frac{dU}{dp}(k\Psi + \delta lX) + \frac{\sigma_e}{f_0}\Omega$$
$$= \frac{\epsilon\,\sigma_e}{f_0} hm^2 E_k \Psi_B \qquad (4.15)$$

$$m^2 X = \frac{d\Omega}{dp}, \qquad (4.16)$$

where $m^2 = k^2 + l^2$. Within the context of the three-level model, we apply the vorticity equation (4.14) at levels 1, 3 and 5 and the thermodynamic equation (4.15) at levels 2 and 4. The boundary conditions are $\Omega_0 = 0$ at the top and $\Omega_6 = m^2 E_k \psi_6$ at the bottom the model which corresponds to the top of the Ekman layer. Using finite differences and linear interpolation between the levels when required, we obtain a system of five equations in the five variables Ψ_1, Ψ_3, Ψ_5, Ω_2 and Ω_4. The streamfunction at the bottom of the model Ψ_6 is obtained by linear extrapolation from Ψ_3 and Ψ_5. The algebraic system is further reduced to three equations by the elimination of Ω_2 and Ω_4 using the thermodynamic equation. The form for $h(p)$ and $g(p)$ can be specified in agreement with the discussion in YC and with the results of a diagnostic study of an explosive east coast storm which occurred on January 20–22, 1979 (Mailhot, 1985). We set

$$g_1 = -1, \qquad g_3 = 0, \qquad g_5 = 1,$$
$$h_0 = h_6 = 0, \qquad h_2 = h_4 = 1.$$

In terms of the non-dimensional numbers

$$\varepsilon' = \frac{\varepsilon f_0}{\Delta p}, \qquad \nu = \frac{l}{\lambda}$$

where

$$\lambda^2 = \frac{f_0^2}{\sigma \Delta p^2}, \qquad (\sigma_e)_2 = (\sigma_e)_4 = \sigma,$$

$$U_j = (6-j)U_T, \qquad \frac{dU}{dp} = -2\frac{U_T}{\Delta p},$$

the linear baroclinic instability problem becomes a simple eigenvalue problem of the form

$$\boldsymbol{A\Psi} = c\boldsymbol{\Psi}, \qquad (4.17)$$

where $\boldsymbol{\Psi} = [\Psi_1, \Psi_3, \Psi_5]^T$ and $\boldsymbol{A}$ is a 3×3 matrix.

Eq. (4.17) can be solved for the three eigenvalues c at fixed wavenumbers either by standard matrix inversion or as a direct solution of a cubic equation. In general, it is found that there is one amplifying mode (i.e., $c_{i1} > 0$), one damped mode ($c_{i2} < 0$) and one neutral mode ($c_{i3} \sim 0$), where c_i refers to the imaginary part of c.

As a typical example, we now present numerical solutions obtained with the following set of parameters

$$U_T = 5\ \mathrm{m\ s^{-1}}, \quad f_0 = 10^{-4}\ \mathrm{s^{-1}}, \quad \beta = 10^{-11}\ \mathrm{m^{-1}\ s^{-1}},$$
$$\lambda = 2.1 \times 10^{-6}\ \mathrm{m^{-1}}, \quad \nu = -0.675, \quad E_k = 16\ \mathrm{mb}.$$

Four situations are considered as is illustrated in Table 1. The values for ϵ and ε' are chosen to yield a magnitude for the recycling rate term and vortex tube stretching term in (4.7) in agreement with scaling arguments in Section 2.

The purely baroclinic case characterized by $\epsilon = 0$ and $\varepsilon' = 0$ will be referred to as case A. The situation where the non-geostrophic effects are excluded but the convection effects are considered (that is $\epsilon, \epsilon' \neq 0$, $\delta = 0$) will be called case B. This case is similar to the case presented in YC. Case C represents the situation when the non-geostrophic effects are included but the recycling rate effect is ignored ($\delta = 1$, $\varepsilon' = 0$). Finally, case D includes all the effects of clouds. These four experiments can best be understood from a consideration of the potential vorticity and omega equations and the related discussion in Section 3. Case B corresponds to a forcing of the potential vorticity by the recycling rate effect only, while the vertical velocity field is forced mainly by the heating and dynamical effects of cumulus clouds. On the other hand, in case C, the two forcing functions arising from non-geostrophic effects are the sole forcing mechanisms for the potential vorticity, while the vertical motion is caused primarily by the two

Table 1. *Values of the different parameters used in the experiments with the three-level model*

Case	δ	ϵ	ε'
A	0	0	0
B	0	10	1
C	1	10	0
D	1	10	1

terms containing M_c (i.e., diabatic heating and vortex stretching by cumulus clouds). Since according to (3.5)–(3.6), the omega field is forced essentially by the same mechanisms in cases B and C, it is clear that these cases differ mainly due to the forcing functions considered in the potential vorticity equation.

Fig. 2 shows the growth rates, expressed in the dimensionless form $kc_i/\lambda U_T$ as a function of the non-dimensional wavenumber k/λ, for the unstable solutions. It is seen that convection increases appreciably the growth rate at all wavenumbers (case D), as compared to the purely baroclinic case (case A), and to reduce slightly the wavelength of the most unstable mode. Note also that the effects of the non-geostrophic terms (case C) are quite similar to the case without these terms (case B), except at larger wavenumbers.

Figs. 3 and 4 present the vertical structure of the most unstable wave, for each of the four cases. The amplitude of the streamfunction is normalized to a maximum value of unity. For the baroclinic case with friction (case A), it is well known that the amplitude has its maximum at the top of the model, with a slight secondary maximum near the surface. In comparison, the amplitude in case B is much larger near the surface, while slightly smaller at 500 mb. In contrast, case C produces a maximum at level 3. Case D represents a combination of the B and C cases. Thus the different effects of clouds can produce significant differences in the vertical structure of the geopotential perturbation.

A comparison of the wave structure for the geopotential, temperature and vertical velocity phases in a west-east cross-section is plotted in Fig. 4. The usual phase relationships for a baroclinically unstable wave are noted in case A. The wave is characterized by a westward tilting of the trough with height and a maximum upward motion slightly ahead of the surface trough. The warm air axis lies farther ahead and tilts eastward as the height increases. Case B shows a similar structure with an enhanced westward tilt of the trough, consistent with the larger growth rate, and a better correlation between the location of upward motion and the warm air ridge. This picture is in agreement with a larger conversion between available potential energy and kinetic energy, resulting in an increased instability of the baroclinic flow. In case C, the most striking feature is the westward tilting of the temperature wave which is also noted in D. It thus seems that the two effects due to cumulus convection considered separately in cases B and C can force quite different wave structures.

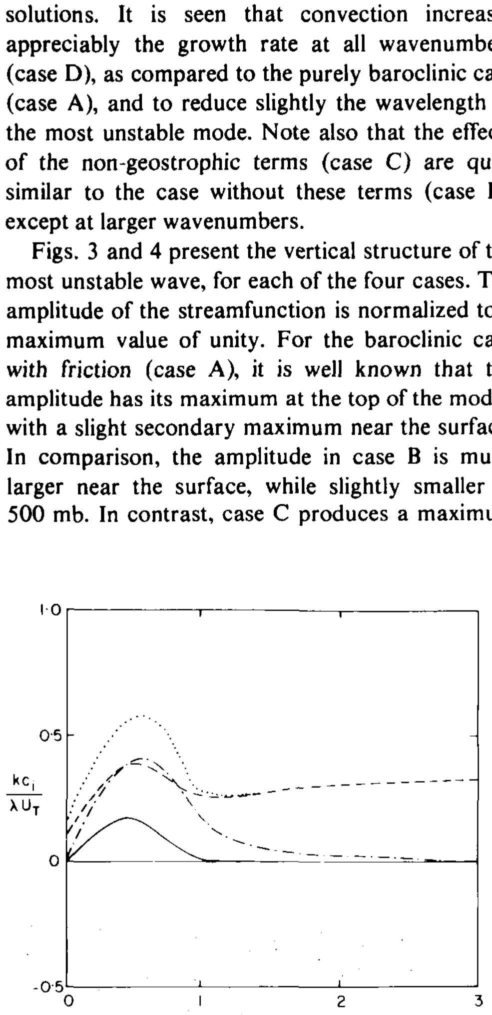

Fig. 2. Non-dimensional growth rate for the most unstable solutions as a function of the non-dimensional zonal wavenumber. Case A (solid line), case B (dashed line), case C (dashed-dotted line), and case D (dotted line). The curves for cases B and D coincide at large wavenumbers.

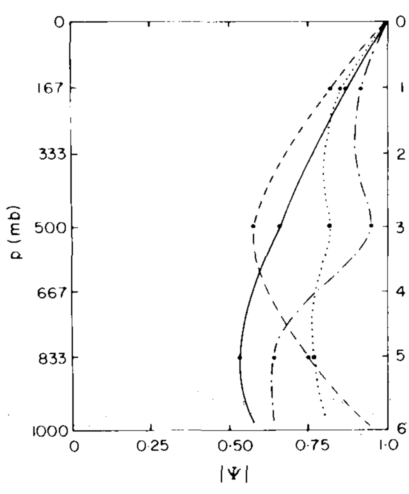

Fig. 3. Vertical distribution of the streamfunction amplitude (normalized to a maximum value of unity) for the most unstable wave. Same key as Fig. 2. The large dots denote the results at the actual levels of the model (Fig. 1), and the continuous lines are obtained by interpolation or extrapolation between these levels.

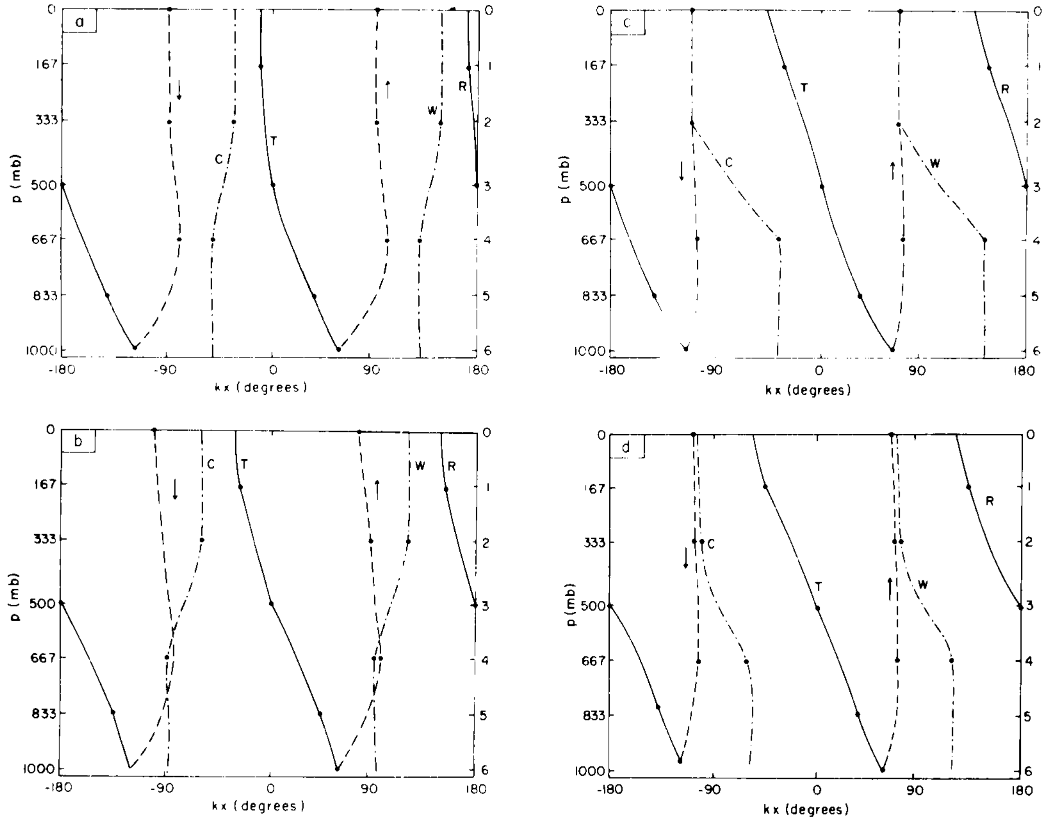

Fig. 4. Vertical and east-west cross-section of the structure of the most unstable wave. (a) Case A, (b) case B, (c) case C, and (d) case D. The height trough and ridge are denoted by T and R, the maximum and minimum in temperature by W and C, and the maximum upward and downward motion by arrows.

It is difficult at this point to relate these features to observed properties of mid-latitude synoptic waves, due to the simplicity of our three-level linear model. A more detailed numerical model is certainly called upon to assess quantitatively these results and to permit realistic comparisons with observations. Nevertheless, the results obtained here indicate that cumulus convection can induce different responses of the large-scale flow as compared to the purely baroclinic case. In reality, the different mechanisms probably operate simultaneously with possibly varying degree of importance during the evolution of the wave.

5. Summary and conclusions

We have investigated in this paper the effects of intense cumulus convection on the dynamics of explosive mid-latitude synoptic-scale storms. A complete set of simplified equations appropriate to these systems was derived through a scale analysis and was used in a linear model of baroclinic instability.

By adopting a scale for the precipitation rate on the order of 10 cm day^{-1} in agreement with observations, it was shown that:

(1) The large diabatic heating by clouds produces a large-scale vertical motion $\bar{\omega}$ on the order of 10^{-2} mb s^{-1}.

(2) The mean vertical motion $\bar{\omega}$ is mainly associated with the vertical mass transport by the cumulus clouds M_c. The averaged vertical velocity in the environment $\tilde{\omega}$ is therefore one order of magnitude smaller than $\bar{\omega}$ and M_c.

(3) The divergent part of the wind is of the same order as the rotational part with a result that

the large-scale divergence can be as large as the large-scale vorticity.

(4) To achieve such a value for $\bar{\omega}$, a 10% cumulus cloud coverage is necessary.

(5) The large-scale divergent wind is mainly caused by the horizontal eddy flux of vertical vorticity. It is associated with a secondary circulation set up by the strong vertical motion from heating in the clouds. The advection by the divergent wind makes important contributions in both the thermodynamic and vorticity equations, and constitutes the basic mechanism by which heating in the clouds influences the large-scale flow.

(6) Despite the effects of clouds, the quasi-geostrophic scaling is still valid for the large-scale non-divergent wind, the vorticity, and the geopotential.

(7) It was shown that the heating effect of the clouds induces a large ageostrophic wind to yield a greater growth rate (Case C). At this moment, it is not possible to isolate the relative effect and physical mechanism of the heating and ageostrophic wind in enhancing the rate of baroclinic energy conversion. Further research in the energetics of baroclinic systems with intense convection will be pursued in the future.

The scale analysis yields a consistent set of equations including the dynamic and thermodynamic effects of clouds. A linear baroclinic instability study using this set of equations in the context of a three-level model indicated that clouds not only increase the growth rate of the most unstable waves but also affect their structures. Further research along this line should include an extension of the results in a multi-level model with realistic basic states. This would allow comparison of theory with observations.

6. Acknowledgments

This work is based on a thesis submitted by J. Mailhot to McGill University in partial fulfillment of the requirements for the Ph.D. degree. Helpful discussions with H. R. Cho and T. Warn are gratefully acknowledged. The research reported here has been supported by the Atmospheric Environment Service of Canada and the National Science and Engineering Research Council of Canada. The authors would like to thank C. Temperton for reviewing the manuscript, and 2 anonymous reviewers for useful suggestions. U. Seidenfuss expertly drafted the figures.

REFERENCES

Arakawa, A. and Schubert, W. H. 1974. Interaction of a cumulus cloud ensemble with the large-scale environment, Part I. *J. Atmos. Sci. 31*, 674–701.

Bosart, L. F. 1981. The President's Day snowstorm of 18–19 February 1979: A subsynoptic scale event. *Mon. Wea. Rev. 109*, 1542–1566.

Charney, J. G. and Eliassen, A. 1964. On the growth of the hurricane depression. *J. Atmos. Sci. 21*, 68–75.

Chen, T. C., Alpert, J. C. and Schlatter, T. W. 1978. The effects of divergent and nondivergent winds on the kinetic energy budget of a mid-latitude cyclone: A case study. *Mon. Wea. Rev. 106*, 458–468.

Cho, H. R. 1977. Contribution of cumulus cloud life-cycle effects to the large-scale heat and moisture budget equations. *J. Atmos. Sci. 34*, 87–97.

Cho, H. R., Cheng, L. and Bloxam, R. M. 1979. The representation of cumulus cloud effects in the large-scale vorticity equation. *J. Atmos. Sci. 36*, 127–139.

Cho, H. R. and Cheng, L. 1980. Parameterization of horizontal transport of vorticity by cumulus convection. *J. Atmos. Sci. 37*, 812–826.

Cho, H. R. and Clark, T. L. 1981. A numerical investigation of the structure of vorticity fields associated with a deep convective cloud. *Mon. Wea. Rev. 109*, 1654–1670.

Danard, M. B. 1964. On the influence of released latent heat on cyclone development. *J. Appl. Meteorol. 3*, 27–37.

Gyakum, J. R. 1983. On the evolution of the QE II storm. II: Dynamic and thermodynamic aspects. *Mon. Wea. Rev. 111*, 1156–1173.

Haltiner, G. J. 1971. *Numerical weather prediction.* Wiley, New York, 317 pp.

Holton, J. R. 1979. *An introduction to dynamic meteorology*, 2nd edition. Academic Press, New York, 391 pp.

Krishnamurti, T. N. 1968. A study of a developing wave cyclone. *Mon. Wea. Rev. 96*, 208–217.

Krishnamurti, T. N. and Moxim, W. J. 1971. On parameterization of convective and non-convective latent heat release. *J. Appl. Meteorol. 10*, 3–13.

Kuo, H. L. 1965. On formation and intensification of tropical cyclones through latent heat release by cumulus convection. *J. Atmos. Sci. 22*, 40–63.

Kuo, H. L. 1974. Further studies of the parameterization of the influence of cumulus convection on large-scale flow. *J. Atmos. Sci. 31*, 1232–1240.

Mailhot, J. 1985. On the effects of cumulus convection on mid-latitude explosive cyclones. McGill University Scientific Report MW-96, 204 pp.

Ooyama, K. 1971. A theory of parameterization of cumulus convection. *J. Meteorol. Soc. Japan 49*, 744–756.

Palmén, E. 1958. Vertical circulation and release of kinetic energy during the development of Hurricane Hazel into an extratropical storm. *Tellus 10*, 1–23.

Riehl, H. and Malkus, J. S. 1958. On the heat balance of the equatorial trough zone. *Geophysica 6*, 503–538.

Sanders, F. and Gyakum, J. R. 1980. Synoptic-dynamic climatology of the "bomb". *Mon. Wea. Rev. 108*, 1589–1606.

Shapiro, L. J. 1978. The vorticity budget of a composite African tropical wave disturbance. *Mon. Wea. Rev. 106*, 806–817.

Shapiro, L. J. and Stevens, D. E. 1980. Parameterization of convective effects on the momentum and vorticity budgets of synoptic-scale Atlantic tropical waves. *Mon. Wea. Rev. 108*, 1816–1826.

Stevens, D. E., Lindzen, R. S. and Shapiro, L. J. 1977. A new model of tropical waves incorporating momentum mixing by cumulus convection. *Dyn. Atmos. Oceans 1*, 365–425.

Tracton, M. S. 1973. The role of cumulus convection in the development of extratropical cyclones. *Mon. Wea. Rev. 101*, 573–593.

Vincent, D. G. and Schlatter, T. W. 1979. Evidence of deep convection as a source of synoptic scale kinetic energy. *Tellus 31*, 493–504.

Yanai, M., Esbensen, S. and Chu, J. H. 1973. Determination of bulk properties of tropical cloud clusters from large-scale heat and moisture budgets. *J. Atmos. Sci. 30*, 611–627.

Yip, T. C. and Cho, H. R. 1982. Dynamics of quasi-geostrophic systems with cumulus convection. *Tellus 34*, 63–73.